



# Characterization of saffron from different origins by HS-GC-IMS and authenticity identification combined with deep learning

Yingjie Lu<sup>a,1</sup>, Chi Zhang<sup>a,b,1</sup>, Kunmiao Feng<sup>a,1</sup>, Jie Luan<sup>c</sup>, Yuqi Cao<sup>d</sup>, Khalid Rahman<sup>e</sup>, Jianbo Ba<sup>c,\*\*</sup>, Ting Han<sup>a,\*\*</sup>, Juan Su<sup>a,b,\*</sup>

<sup>a</sup> School of Pharmacy, Naval Medical University, Shanghai 200433, China

<sup>b</sup> National Demonstration Center for Experimental Military Pharmacy Education, Naval Medical University, Shanghai 200433, China

<sup>c</sup> Naval Medicine Center of PLA, Naval Medical University, Shanghai 200433, China

<sup>d</sup> Technical Centre, Shanghai Tobacco (Group) Corp., Shanghai 200082, China

<sup>e</sup> Faculty of Science, School of Pharmacy and Biomolecular Sciences, Liverpool John Moores University, Liverpool, United Kingdom

## ARTICLE INFO

### Keywords:

Saffron  
Volatile components  
Convolutional neural networks  
HS-GC-IMS  
Origins

## ABSTRACT

With the rising demand of saffron, it is essential to standardize the confirmation of its origin and identify any adulteration to maintain a good quality led market product. However, a rapid and reliable strategy for identifying the adulteration saffron is still lacks. Herein, a combination of headspace-gas chromatography-ion mobility spectrometry (HS-GC-IMS) and convolutional neural network (CNN) was developed. Sixty-nine volatile compounds (VOCs) including 7 groups of isomers were detected rapidly and directly. A CNN prediction model based on GC-IMS data was proposed. With the merit of minimal data preprocessing and automatic feature extraction capability, GC-IMS images were directly input to the CNN model. The origin prediction results were output with the average accuracy about 90 %, which was higher than traditional methods like PCA (61 %) and SVM (71 %). This established CNN also showed ability in identifying counterfeit saffron with a high accuracy of 98 %, which can be used to authenticate saffron.

## 1. Introduction

Saffron is the stigma of *Crocus sativus* L, which is a traditional Mediterranean plant belonging to the Family Iridaceae. As an edible herb cultivated globally, saffron is widely used as a condiment and medicine. (Pandita, 2021) It has been reported that saffron not only possess the effects of antispasmodic, antiseptic, anti-fungal etc. (Avgerinos et al., 2020), but can also be used as a flavoring agent in cosmetics, agricultural products and food items (Ahrazem, Rubio-Moraga, Nebauer, Molina, & Gómez-Gómez, 2015). The geographical cultivation area of saffron is around the Mediterranean countries and Asian countries include Iran, Italy, Spain, India, China, Greece, and Morocco (Kumar, Devi, Kumar, & Kumar, 2022). Due to the different growing environment and cultivation method, saffron possess diverse characteristics. Among them, the unique composition of volatile components and the

changes in flavor are the critical indicators for evaluating its quality (Maggi et al., 2010) However, it is hard to accurately identify saffron from different origins by means of human olfaction alone. This phenomenon poses a great challenge for the identification and adulteration of saffron in a rapid way. Hence, a rapid and reliable method is necessary for investigating the discrepancies in aroma compounds of saffron from different origins.

Currently, several methods have been developed for the identification and authentication of saffron including ultra-high performance liquid chromatography (Rubert, Lacina, Zachariasova, & Hajslova, 2016), mid-infrared spectroscopy and near-infrared spectroscopy (Amirvaresi, Nikounezhad, Amirahmadi, Daraei, & Parastar, 2021), high-performance thin-layer chromatography (Amirvaresi et al., 2020) and so on. However, the resolution of infrared chromatography and chromatography may not detect all the compounds. Aroma is one of the

**Abbreviations:** HS-GC-IMS, headspace-gas chromatography-ion mobility spectrometry; CNN, convolutional neural network; VOCs, volatile compounds; PCA, Principal Component Analysis; SVM, support vector machine.

\* Corresponding author at: School of Pharmacy, Naval Medical University, Shanghai 200433, China.

\*\* Corresponding authors.

E-mail addresses: [bevon@126.com](mailto:bevon@126.com) (J. Ba), [hanting@smmu.edu.cn](mailto:hanting@smmu.edu.cn) (T. Han), [juansu\\_2008@126.com](mailto:juansu_2008@126.com) (J. Su).

<sup>1</sup> These authors contributed equally to this work.

<https://doi.org/10.1016/j.fochx.2024.101981>

Received 29 August 2024; Received in revised form 4 November 2024; Accepted 6 November 2024

Available online 13 November 2024

2590-1575/© 2024 The Authors. Published by Elsevier Ltd. This is an open access article under the CC BY-NC-ND license (<http://creativecommons.org/licenses/by-nc-nd/4.0/>).

important characteristics of saffron and is important for estimating the food's properties related to nutrition, governing food quality and consumer perception. Researchers have contributed to identifying the adulteration of saffron with volatile compounds based on optical (Masoomi, Sharifi, & Hemmateenejad, 2024), proton transfer reaction time-of-flight mass spectrometry (Ghanbari, Khajoei-Nejad, Erasmus, & van Ruth, 2019), and gas chromatography mass spectrometry (GC-MS) (Di Donato, D'Archivio, Maggi, & Rossi, 2021). Among them, GC-MS is one of the most prevalent analytical methods to characterize volatile compounds due to its efficient separate ability. Generally, procedures of extraction and separation are needed before detection by GC-MS and temperature is one of the key factors in determining the dissolution of volatile components from saffron (Kumari, Jaiswal, & Tripathy, 2021). However, excessively high extraction and separation temperatures may lead to the loss of some volatile components that cannot be detected by GC-MS. For this reason, a systematic strategy with little sample pre-treatment process for identifying saffron based on the characteristics of its aromatic components is required.

Headspace-gas chromatography-ion mobility spectrometry (HS-GC-IMS) is an emerging analytical technology with high sensitivity and high separation efficiency for detecting volatile organic compounds (VOCs). Little extraction step for enriching VOCs is one of the most important advantages of HS-GC-IMS. (Brendel, Schwolow, Rohn, & Weller, 2021) The volatilization happens under softer conditions in HS than that in direct injection (Aspromonte, Giacompo, Wolfs, & Adams, 2020). This property may reduce the loss of volatile components during high-temperature extraction process. This method possessed the ability of detecting volatile compounds in a faster, more accurate and sensitive way. At present, HS-GC-IMS has been widely used to detect VOCs in drug analysis (Denia, Esteve-Turrillas, & Armenta, 2022), food flavor identification (Li et al., 2019), traditional medicine detection (Zhou et al., 2022) and other fields. More specifically in the application of food quality evaluation, HS-GC-IMS has been widely utilized to detect and analyze VOCs of food product in a rapid and non-destructive way. (Ge et al., 2020; Li et al., 2019; Pu et al., 2020; Pu et al., 2025; Zhou et al., 2023) HS-GC-IMS has exhibited its advantages in investigating the effect of storage, procession, distribution, growth on flavor change, which have been successfully applied to adulteration and classification in the field of food research. (Gu, Zhang, Wang, Wang, & Du, 2021; Leng, Hu, Cui, Tang, & Liu, 2021; Maggi et al., 2010).

Saffron contains multiple kinds of VOCs and the type and abundance of these compounds significantly affects the aroma and flavor of saffron, which in turn determines its quality. It has been reported that saffron from different geographical areas has been analyzed to investigate whether VOCs can be served as the markers for identifying its origin. (Anastasakis et al., 2009; D'Archivio, Di Pietro, Maggi, & Rossi, 2018; Karabagias, Koutsoumpou, Liakou, Kontakos, & Kontominas, 2017; Naim et al., 2023; Sobolev et al., 2014) These studies have greatly promoted the possibility of using VOCs as differential metabolites to distinguish saffron origins. However, comprehensive preprocessing was needed in these studies and saffron samples from China were not investigated in the current investigations. Especially, saffron from different provinces in China are cultivated with different methods including one-stage planting and two-stage planting. (Chen, Wang, Zhao, Yuan, & Wang, 2003) Therefore, a universal and rapid method is needed for illustrating the possible reason of quality variations by VOCs in saffron from different origins.

In addition to the above-mentioned chemical-based analytical methods, deep learning strategies such as convolutional neural networks (CNN) have also been used as powerful tools in the analysis of complicated data. CNN has shown great potential in the field of classification (Rawat & Wang, 2017) due to the advantage of minimal data preprocessing and accurate automatic feature extraction capability. Herein, inspired by previous works, a strategy based on HS-GC-IMS with CNN was used for the characterization and authentication of saffron. Fifteen saffron samples from 8 different cultivated areas were selected to detect

the VOCs contained under an optimized incubation temperature of HS-GC-IMS. With the application of the established strategy, 7 groups of isomers were obtained. Hierarchical clustering and correlation analysis were used to analyze the fingerprint profiles of VOCs in saffron from different origins. The established CNN model also showed its high prediction accuracy of 90 % in identifying saffron origins and of 98 % in authenticating counterfeit saffron. In summary, the method proposed here might offer inspirations for the identification of saffron origins and authenticity, as well as provided data supports for further studies of VOCs in saffron.

## 2. Materials and methods

### 2.1. Samples

Fifteen dried saffron samples from eight cultivars were gathered from different growing areas. The cultivars from China included Bozhou saffron (BZ), Jiande saffron (JD), Yancheng saffron (YC), Baoding saffron (BD) and Chongming saffron (CM). Among them, the cultivation method of saffron from Chongming are "two-stage planting". In addition, saffron from Iran (Iran-Shiraz, Iran-Kerman) and Spain saffron were collected, which belonged to the "one-stage planting" area. Five fake samples: safflower (SAFFLOWER), Corn Stigma (CORN), saffron's stamen (XR), the mixture of saffron and corn stigma (HH), an unknown plant (WP). 5 fake samples were bought from local providers in Bozhou, China and the botanical identification was confirmed by expert botanists.

### 2.2. HS-GC-IMS analysis

An Agilent 490 gas chromatograph (Agilent Technologies), IMS instrument (FlavourSpec<sup>®</sup>, Gesellschaft für Analytische Sensor systeme mBH, G.A.S., Dortmund, Germany) and an sampling device were implied automatically to identify the aroma compounds in saffron. Approximately 0.15 g of saffron was stored in the 20 mL vial for HS samples and filled in the automatic sampler's tank. The sample was incubated for 10 min in an incubator and the incubation temperature was set to 40 °C, 50 °C, 60 °C, 70 °C, 80 °C for optimization. The injection method was headspace sampling, and oscillate at 500 rpm. The injection volume was set at 500 µL and flushed for 1 min during the injection cycle in order to avoid condensation effects.

The gas chromatography column's temperature was set at 60 °C. Nitrogen (purity ≥99.99 %) was applied both as a carrier gas and drift gas for GC and IMS. The carrier gas flow rate was performed as follows: Initial flow rate at 2.0 mL/min for 2 min, then ascend to 10 mL/min and hold for 8 min, followed by 50 mL/min for 10 min and 100 mL/min for 10 min totally the program was run for 30 min. For IMS, a <sup>3</sup>H-radioactive ionization source and a drift tube (length: 98 mm) was performed at 60 °C with 5 kV drift voltage. The drift gas flow rate was set at 150 mL/min constantly for the whole process and positive ion was applied to the ionization mode.

### 2.3. Convolutional neural network model training

The convolutional neural network model established in this work was based on pytorch. Our CNN model received the GC-IMS fingerprints of saffron as input and returned the possibility of each origin class as output. The model architecture consisted of two main parts: a convolutional layer stack and a classifier. In the convolutional layer stack part, two convolutional layers were with 256 filters each, kernel size was set to (3,3), the activation function was ReLU, and padding set to 'same'. A max-pooling layer was with a pool size of (64, 64) and strides of (64, 64). The input shape for the first convolutional layer was (224, 224, 3), representing an image with height, width, and three-color channels. In the classifier part, a flattening layer was built to convert the output of the convolutional layers into a 1D tensor. Two fully connected (dense)

layers with 512 and 256 units were both activated by using hyperbolic tangent (tanh). A dropout layer with a dropout rate of 0.5 was applied to prevent overfitting. A final dense layer with 9 units and SoftMax activation was suitable for multi-class classification tasks. Codes of this program could be downloaded from <https://github.com/CaoyuqiChemistry/xihonghuaML>.

## 2.4. Statistical analysis

For the initial data obtained from analytical equipment following software was used: (i) Laboratory Analytical Viewer (LAV) software was applied to reveal the analytical spectrum and set up a standard curve to quantify the plots which represent different VOCs; (ii) Reporter plug-in showed two-dimensional (2D) contour plots of each sample; (iii) The GC-IMS fingerprints was plotted by Gallery plot plug-in; (iv) The GC-IMS Library search software compiled of NIST (National Institute of Standards and Technology) and IMS databases showed the qualitative analysis of substances; (v) The hierarchical clustering analysis (HCA) was performed by Origin 2021 software; (vi) The workflow of the generation of the heatmap followed 3 steps. Firstly, the peak volume of each VOC was extracted by the Vocal software. Then, the peak volume value of each VOC was calculated from the topographic plots. Secondly, Pearson correlation coefficient matrix was obtained by the acquired peak volume value of all VOCs from 8 different saffron origins. Finally, the correlation heatmap was visualized by the generated heatmap.

## 3. Results and discussion

### 3.1. Optimizing incubation temperature of VOCs analysis by HS-GC-IMS

The evaporation of aroma compounds in saffron is temperature-dependent. As the temperature become higher, the more volatile compounds escape from saffron. In order to obtain as many VOCs as possible, the incubation temperature of saffron by HS-GC-IMS was optimized first. A series of temperature was set to 40 °C, 50 °C, 60 °C, 70 °C and 80 °C. Given that Chongming is the main production area of saffron in China, the saffron samples gathered from Chongming Island (Shanghai, China) were taken as the example for detection by HS-GC-IMS. Chemical morphology was used to reveal the analytes detected with different incubation temperature. The principle of HS-GC-IMS applies the fast ion-molecular reaction between air clusters and analytes generated by beta ionization is applied as an indicator of different aromas (Feng, Wang, He, & Tang, 2021). Distinguishing volatile compounds in saffron is based on the national institute of standards and technology (NIST), retention indexes, retention times and drift times (Yang, Wang, Fu, &

Zhang, 2021). Fig. 1 showed 5 different kinds of small-molecule aroma compounds (aldehydes, esters, terpenes, alcohols and ketones) detected under 5 incubation temperatures. When the incubation temperature was set up to 80 °C, the variety of compounds detected was the richest: 7 aldehydes, 7 esters, 8 terpenes, 9 alcohols and 6 ketones. Saffranal, the most representative VOC in saffron, showed the highest intensity under 80 °C. For esters, one more was found under 70 °C and two more were found under 60 °C. This result might probably indicate that higher incubation temperatures could cause the decomposition of esters. VOCs were the same when the temperature was set to 40 °C and 50 °C, which indicated that lower temperatures have little effect on the results.

Fig. S-1 showed specific information of VOCs in fingerprint. As shown in Fig. S-1B, blue means background's color of the spectrum, the abscissa indicates the drift time and the vertical coordinate indicates the retention time (Sun et al., 2019). Each dot on the RIP's (reactant ion peak) right side indicated the chemical components identified in saffron. The concentration of VOCs is shown in different colors, which were based on the signal intensity. Different hues indicated different concentrations, red means higher signal strength, and white means lower signal strength, consequently the brighter the color, the higher the concentration. As shown in Fig. S-1B the majority of the signals appeared at a 150–1200 s measurement run time and 1.0–2.0 s drift time. These five parallel graphs are T1 (40 °C), T2 (50 °C), T3 (60 °C), T4 (70 °C), T5 (80 °C). According to the results, 80 °C was chosen as the incubation temperature so that the saffron samples volatilized with the largest variety of aroma compounds.

### 3.2. HS-GC-IMS topographic plots of saffron from different origins

HS-GC-IMS has been used to detect the VOCs in saffron flowers (stigmas, stamens, and tepals), which has promoted the study in saffron. In our work, the profiling of VOCs in saffron from different areas was conducted by HS-GC-IMS with the optimized incubation temperature of 80 °C. As shown in Fig. 2A, the two-dimensional vertical view spectra of saffron from 8 different origins were obtained by Reporter plugin. The background color of the two-dimensional vertical view spectra was blue. The horizontal axis represents the retention time of gas chromatography. The vertical axis represents the drift time of the ion migration spectrum. The highest signal peak at 1.0 in the horizontal coordinate and at each point in the vertical coordinate indicates the normalized reactive ion peaks. Fig. 2A showed that practically all VOCs were detected between 100 and 1200 s. Different colors in each two-dimensional vertical view spectra represented different VOCs observed in saffron. And the diverse fingerprints might reflect the unique composition and various concentration of VOCs. According to the colorbar shown in Fig. 2A, the closer the color was to red represented the higher the concentration of VOCs detected in saffron. Correspondingly, the closer the color was to black represented the lower the concentration of VOCs detected in saffron.

In order to explore the variation among VOCs in saffron from different origins through a more intuitive way, a differential comparison tool was utilized to visualize the differences at molecule level. The spectrum of saffron from Chongming (CM) was chosen as a reference. As shown in Fig. 2B the difference spectra were obtained by the other 7 spectra of saffron samples from 7 origins minus the CM spectrum. When the background color was closer to white after subtraction, it means that the concentration of VOCs detected was very close to each other. Correspondingly, if the color was closer to dark blue mean a lower content in the specific origin of saffron than that in CM. If the color was closer to red mean a higher content in the specific origin of saffron than that in CM. The closer the color is to the extremes, the greater the difference represents. Significant differences could be observed between the drift time from 1.0 to 1.5 ms and retention time 50–100 s, the drift time from 1.2 to 1.7 ms and retention time 750–900 s. Among the above-mentioned measured times, the VOCs in saffron from CM showed the lower content than those from Iran-Shiraz, Bozhou, Jiande, Baoding and

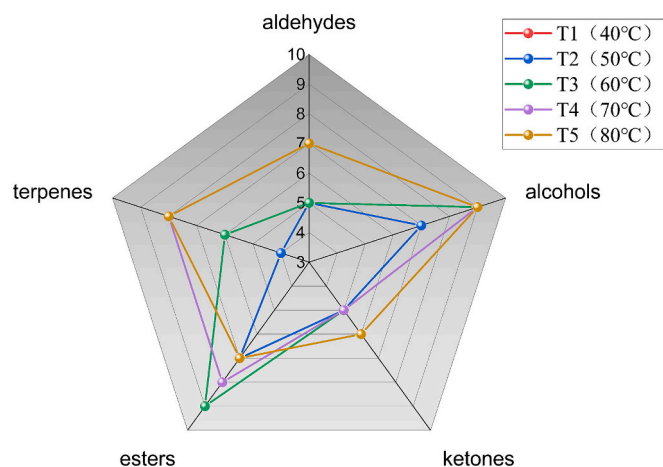
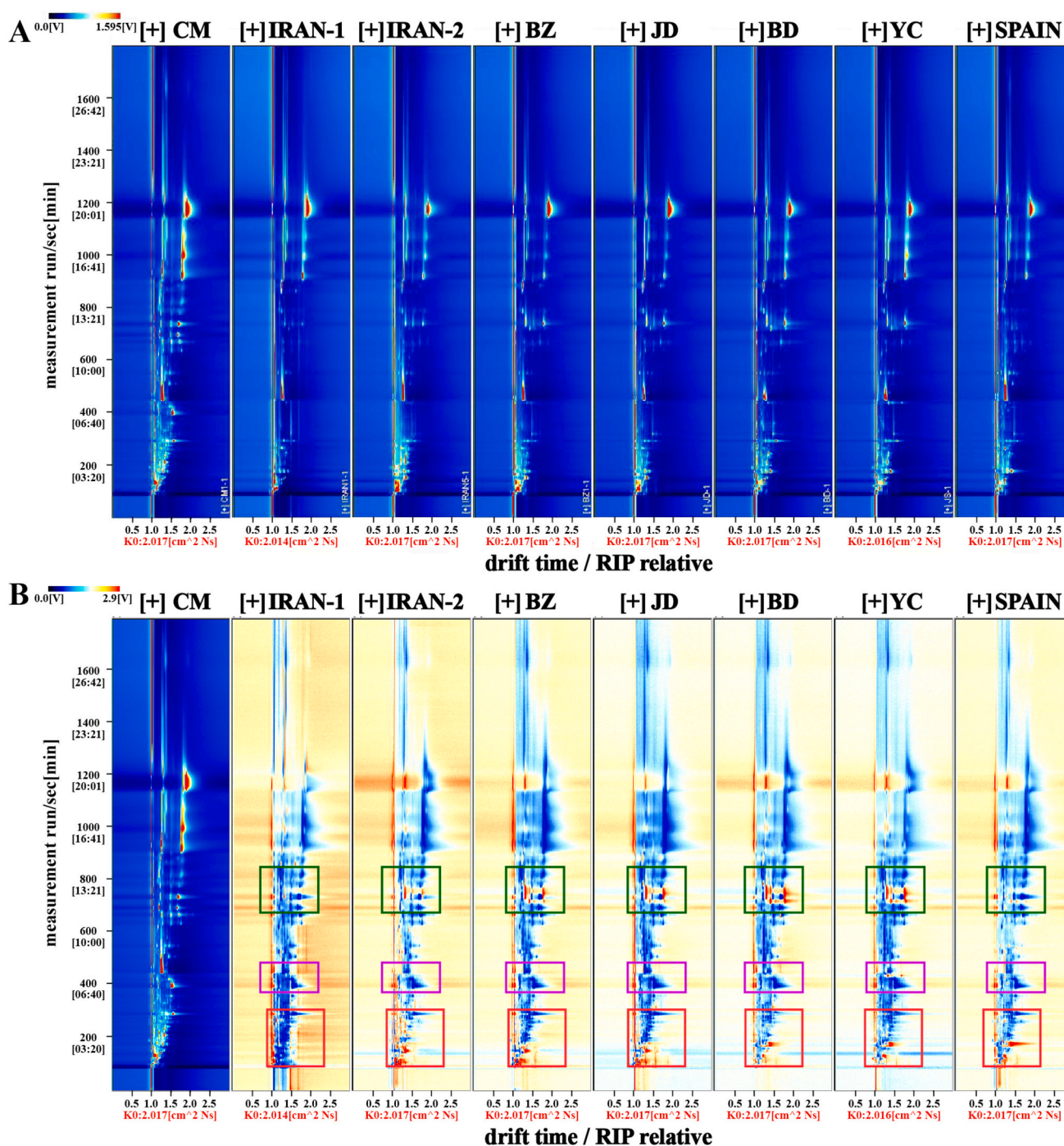


Fig. 1. Radar chart of detected VOCs in saffron with different incubation temperatures.





**Fig. 2.** (A) 2D Topographical map of saffron from different origins; (B) Differential spectra of saffron samples with saffron from Chongming as a reference.

Yancheng. However, the saffron from Iran-Kerman and Spain, the VOCs in saffron from CM showed a higher content. The difference spectra from the seven origins also showed interesting similarities and differences with each other. The difference spectra from Baoding and Yancheng displayed a high similarity in terms of concentration and VOCs type. This phenomenon could also be observed in the differential spectra from Bozhou and Jiande. In contrast, saffron samples from different origins in Iran in the drift time of 100–400 ms and 750–800 ms showed obvious difference. These results indicated that saffron from different areas of the same country possessed diverse VOCs profiles, which might be closely related to the elements including cultivation method, growth climate, natural conditions. With the utilizing of HS-GC-IMS, the topographic plots of saffron could provide reliable information for the

evaluation of the saffron quality.

### 3.3. Identification and differential analysis of VOCs in saffron from different origins

The aroma of saffron mainly depended on the concentration and composition of the contained volatile components. The concentration and composition of VOCs detected were closely related to the origins of saffron. In this work, semi-quantitative analysis with the signal height and volume data has been carried out for obtaining the differences in VOCs from 8 different saffron origins. Besides, the Gallery Plot plugin has been used to extract each peak signal annotated from the topographical map. As shown in Fig. 3, the fingerprint spectrum was

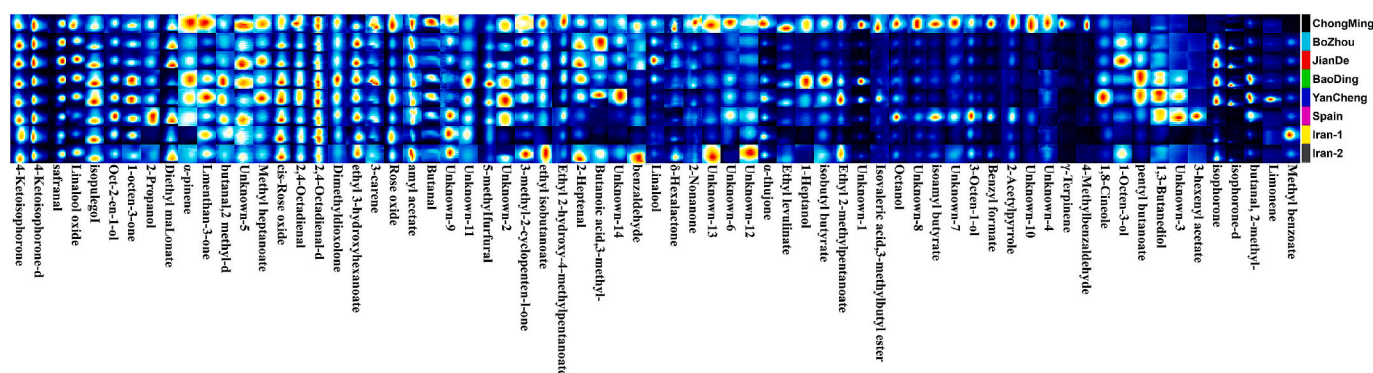


**Fig. 3.** The fingerprint of VOCs detected in 8 different origins.

established by 69 detected peak signals including 55 identified compounds and 14 unidentified compounds. Each point in the fingerprint spectrum represented one volatile compound. And the color of each point is positively correlated with the concentration of each volatile compound. The brighter the color, the higher the content of VOC contained in saffron. Correspondingly, the darker the color, the lower the content of VOC contained in saffron. The vertical columns in the fingerprint spectrum represented each volatile component and the horizontal columns represented each origin. Peaks of volatile compound dimer were appeared, which might be attributed to the high content in saffron sample or strong proton affinity (Capitain & Weller, 2021).

According to the results in the fingerprint spectrum, 4-ketoisophorone, oct-2-en-1-ol, cis-rose oxide, ethyl 3-hydroxyhexanoate showed little difference in peak signal intensity among 8 different origins. Twenty-three VOCs (safranal, linalool oxide, isopulegol, 5-methylfurfural, 2-propanol, diethyl malonate, 3-carene, butanal, L-menthan-3-one, 2,4-octadienal, alpha-pinene, rose oxide, butanal 2-methyl, amyl acetate, dimethyldioxolone, ethyl 2-hydroxy-4-methylpentanoate, isobutyl butyrate, 1-octen-3-one, 2-heptenal, alpha-thujone, 2-nonanone, delta-hexalactone and methyl heptanoate) could be detected in all 8 origins but showed the variation in concentration. Other VOCs showed exhibit particularly high signal intensity in certain saffron origins. For example, several VOCs showed relatively high content in saffron from Chongming including gamma-terpinene, ethyl levulinate, octanol, 4-methylbenzaldehyde, benzyl formate and isovaleric acid 3-methylbutyl ester. Besides, other VOCs exhibited the highest signal intensity in other specific origins, such as limonene, 1,8-cineole and 1,3-butanediol in Yancheng saffron, 1-heptanol, isoamyl butyrate and dimethyldioxolone in Baoding saffron, methyl benzoate in Iran-Kerman, 3-octen-1-ol and 3-hexenyl acetate in Spain saffron, 3-methyl-2-cyclopenten-1-one in Iran-Shiraz saffron. In addition, some VOCs could be detected in several saffron origins and showed different intensities. For example, isophorone could be detected in Bozhou, Jiande, Baoding, Yancheng and Iran saffron, of which Iran saffron showed the lowest intensity. 1-octen-3-ol could not be detected in Iran-Kerman saffron and showed the highest intensity in Jiande saffron. Ethyl isobutanoate could not be detected in Iran-Kerman saffron and showed the highest intensity in Iran-Shiraz saffron. Ethyl 2-methylpentanoate could not be detected in Iran-Kerman saffron and showed the highest intensity in Yancheng saffron. Pentyl butanoate could not be detected in Chongming saffron and showed the highest intensity in Baoding saffron. 3-methyl-butanoic acid could not be detected in Spain and Iran-Kerman saffron, and showed the highest intensity in Bozhou saffron. Benzaldehyde could not be detected in Iran-Kerman saffron, but showed the highest intensity in Iran-Shiraz saffron. These surprising findings may provide a viable strategy for identifying VOC characteristics of saffron from different origins.

The specific information of the detected 69 peaks are summarized in [Table 1](#). With the equipment of IMS for extending the time of VOC ions in drift tubes, several isomers could be identified with the

multidimensional data information including ion drift times, retention times, and peak intensities. Isomers are compounds with the same molecular formula and different structures, also known as structural isomers. Due to the same molecular weight, isomer brought out significant challenges when using other analytical techniques such as MS for detection. In this work, 7 groups of isomers were obtained by HS-GC-IMS (Table S-1): 1) oct-2-en-1-ol, 3-octen-1-ol and 1-octen-3-ol; 2) gamma-terpinene, 3-carene, limonene and alpha-pinene; 3) isopulegol, L-menthan-3-one, rose oxide, linalool, cis-rose oxide, and 1,8-cineole; 4) ethyl 3-hydroxyhexanoate and ethyl 2-hydroxy-4-methylpentanoate; 5) ethyl 2-methylpentanoate, isobutyl butyrate, and methyl heptanoate; 6) methyl benzoate and benzyl formate; 7) pentyl butanoate and isoamyl butyrate. Among the above-mentioned groups of isomers, oct-2-en-1-ol and 3-octen-1-ol possessed the close retention times, while the different ion drift times could distinguish them with each other. Gamma-terpinene and limonene, ethyl 3-hydroxyhexanoate and ethyl 2-hydroxy-4-methylpentanoate, isobutyl butyrate, and methyl heptanoate possessed the similar ion drift times, while the diverse retention times could discriminate isomers. Therefore, HS-GC-IMS has the potential to provide strong technical support for exploring more VOCs in saffron from different regions.

### 3.4. Clustering and correlation analysis of VOCs in saffron from different origins

Hierarchical cluster analysis (HCA) was performed for further investigating the potential similarities and differences of VOCs in saffron samples from different origins. As a multivariate statistical analysis technique, the heatmaps and dendrograms of HCA can also intuitively reflect the correlations among VOCs and the classification of saffron origins. The normalized data used for clustering analysis were obtained from the signal intensities of VOCs in the spectra detected by HS-GC-IMS. Fig. 4A visualized the variation of VOCs in saffron from different origins. Each square in the semicircle represented one compound detected, and the concentric circles with openings labeled from different origins of saffron. According to the color bar, the red color represented a high concentration and the green color represented a low concentration. As shown in Fig. 4A, most VOCs in saffron sample from Chongming possessed a higher content than those in other saffron samples from other 7 origins. Except for 4 VOCs, isophorone, methyl benzoate, 2-methyl-butanol and limonene, showed a relatively low concentration in saffron from Chongming. In addition, comparative strong similarities were observed between origins from Bozhou and Jiande, Yancheng and Baoding. Especially in saffron samples from Baoding and Yancheng, VOCs including pentyl butanoate, 2-methyl-butanol, 2,4-octadienal, ethyl levulinate, butanol, ethyl 3-hydroxyhexanoate, isobutyl butyrate and 1-heptanol showed a higher concentration than those in Bozhou and Jiande. When it comes to origins from Iran Shiraz and Kerman, significant difference could be observed in VOCs of 3-methyl-butanoic acid, 1-

**Table 1**

VOCs detected by HS-GC-IMS from saffron samples from different origins.

NO.	Compound	CAS#	Molecular formula	MW	RI	Rt [sec]	Dt [a.u.]
1	isophorone	C78591	C <sub>9</sub> H <sub>14</sub> O	138.2	1084.0	749.7	1.307
2	isophorone-d	C78591	C <sub>9</sub> H <sub>14</sub> O	138.2	1083.2	744.3	1.763
3	4-ketoisophorone	C1125219	C <sub>9</sub> H <sub>12</sub> O <sub>2</sub>	152.2	1134.7	1182.9	1.320
4	4-ketoisophorone-d	C1125219	C <sub>9</sub> H <sub>12</sub> O <sub>2</sub>	152.2	1134.5	1180.2	1.882
5	2-methyl-butanal	C96173	C <sub>5</sub> H <sub>10</sub> O	86.1	912.3	171.8	1.179
6	2-methyl-butanol-d	C96173	C <sub>5</sub> H <sub>10</sub> O	86.1	917.1	178.8	1.397
7	2,4-octadienal	C30361285	C <sub>8</sub> H <sub>12</sub> O	124.2	1108.1	930.8	1.264
8	2,4-octadienal-d	C30361285	C <sub>8</sub> H <sub>12</sub> O	124.2	1115.9	999.2	1.810
9	oct-2-en-1-ol	C18409171	C <sub>8</sub> H <sub>16</sub> O	128.2	1050.6	555.1	1.145
10	3-octen-1-ol	C20125842	C <sub>8</sub> H <sub>16</sub> O	128.2	1050.8	555.9	1.350
11	1-octen-3-ol	C3391864	C <sub>8</sub> H <sub>16</sub> O	128.2	988.4	319.2	1.579
12	gamma-terpinene	C99854	C <sub>10</sub> H <sub>16</sub>	136.2	1071.9	672.1	1.686
13	3-carene	C13466789	C <sub>10</sub> H <sub>16</sub>	136.2	999.2	349.4	1.203
14	limonene	C138863	C <sub>10</sub> H <sub>16</sub>	136.2	1025.4	442.6	1.692
15	alpha-pinene	C7785708	C <sub>10</sub> H <sub>16</sub>	136.2	931.1	200.3	1.293
16	isopulegol	C89792	C <sub>10</sub> H <sub>18</sub> O	154.3	1124.1	1074.9	1.382
17	L-menthan-3-one	C14073973	C <sub>10</sub> H <sub>18</sub> O	154.3	1124.7	1081.0	1.866
18	rose oxide	C16409431	C <sub>10</sub> H <sub>18</sub> O	154.3	1107.4	925.5	1.779
19	linalool	C78706	C <sub>10</sub> H <sub>18</sub> O	154.3	1103.6	893.8	1.684
20	cis-rose oxide	C3033236	C <sub>10</sub> H <sub>18</sub> O	154.3	1116.5	1003.8	1.340
21	1,8-cineole	C470826	C <sub>10</sub> H <sub>18</sub> O	154.3	1025.6	443.2	1.335
22	ethyl 3-hydroxyhexanoate	C2305251	C <sub>8</sub> H <sub>16</sub> O <sub>3</sub>	160.2	1131.7	1151.0	1.300
23	ethyl 2-hydroxy-4-methylpentanoate	C10348477	C <sub>8</sub> H <sub>16</sub> O <sub>3</sub>	160.2	1065.7	636.0	1.289
24	ethyl isobutanoate	C97621	C <sub>6</sub> H <sub>12</sub> O <sub>2</sub>	116.2	931.8	201.5	1.191
25	ethyl 2-methylpentanoate	C39255328	C <sub>8</sub> H <sub>16</sub> O <sub>2</sub>	144.2	938.6	212.9	1.324
26	isobutyl butyrate	C539902	C <sub>8</sub> H <sub>16</sub> O <sub>2</sub>	144.2	956.9	247.0	1.351
27	methyl heptanoate	C106730	C <sub>8</sub> H <sub>16</sub> O <sub>2</sub>	144.2	1033.6	476.4	1.357
28	methyl benzoate	C93583	C <sub>8</sub> H <sub>8</sub> O <sub>2</sub>	136.1	1100.6	870.3	1.602
29	benzyl formate	C104574	C <sub>8</sub> H <sub>8</sub> O <sub>2</sub>	136.1	1041.9	513.1	1.442
30	pentyl butanoate	C540181	C <sub>9</sub> H <sub>18</sub> O <sub>2</sub>	158.2	1079.9	722.3	1.422
31	isoamyl butyrate	C106274	C <sub>9</sub> H <sub>18</sub> O <sub>2</sub>	158.2	1056.5	585.4	1.398
32	5-methylfurfural	C620020	C <sub>6</sub> H <sub>6</sub> O <sub>2</sub>	110.1	988.6	319.9	1.474
33	3-methyl-butanoic acid	C503742	C <sub>5</sub> H <sub>10</sub> O <sub>2</sub>	102.1	881.8	135.3	1.193
34	diethyl malonate	C105533	C <sub>7</sub> H <sub>12</sub> O <sub>4</sub>	160.2	1029.5	459.1	1.235
35	1-octen-3-one	C4312996	C <sub>8</sub> H <sub>14</sub> O	126.2	980.1	298.3	1.263
36	2-propanol	C67630	C <sub>3</sub> H <sub>8</sub> O	60.1	966.4	266.9	1.081
37	2-heptenal	C18829555	C <sub>7</sub> H <sub>12</sub> O	112.2	966.7	267.5	1.247
38	butanal	C123728	C <sub>4</sub> H <sub>8</sub> O	72.1	857.5	113.5	1.114
39	alpha-thujone	C546805	C <sub>10</sub> H <sub>16</sub> O	152.2	1116.1	1000.3	1.846
40	ethyl levulinate	C539888	C <sub>7</sub> H <sub>12</sub> O <sub>3</sub>	144.2	1064.3	628.1	1.175
41	benzaldehyde	C100527	C <sub>7</sub> H <sub>6</sub> O	106.1	921.3	184.9	1.164
42	1-heptanol	C111706	C <sub>7</sub> H <sub>16</sub> O	116.2	931.5	200.9	1.418
43	amyl acetate	C628637	C <sub>7</sub> H <sub>14</sub> O <sub>2</sub>	130.2	914.1	174.3	1.308
44	octanol	C111875	C <sub>8</sub> H <sub>18</sub> O	130.2	1051.0	557.0	1.463
45	2-nonanone	C821556	C <sub>9</sub> H <sub>18</sub> O	142.2	1070.5	663.7	1.406
46	3-methylbutyl ester isovaleric acid	C659701	C <sub>10</sub> H <sub>20</sub> O <sub>2</sub>	172.3	1105.8	912.0	1.479
47	delta-hexalactone	C823223	C <sub>6</sub> H <sub>10</sub> O <sub>2</sub>	114.1	1083.9	748.9	1.515
48	3-hexenyl acetate	C3681718	C <sub>8</sub> H <sub>14</sub> O <sub>2</sub>	142.2	1016.1	406.9	1.322
49	1,3-butanediol	C107880	C <sub>4</sub> H <sub>10</sub> O <sub>2</sub>	90.1	879.2	132.8	1.117
50	3-methyl-2-cyclopenten-1-one	C2758181	C <sub>6</sub> H <sub>8</sub> O	96.1	978.2	293.9	1.407
51	4-methylbenzaldehyde	C104870	C <sub>8</sub> H <sub>8</sub> O	120.2	1076.4	700.3	1.196
52	2-acetylpyrrole	C1072839	C <sub>6</sub> H <sub>7</sub> NO	109.1	1065.5	634.5	1.494
53	dimethyldioxolone	C37830903	C <sub>5</sub> H <sub>6</sub> O <sub>3</sub>	114.1	953.2	239.8	1.166
54	safranal	C116267	C <sub>10</sub> H <sub>14</sub> O	150.2	1102.6	886.4	1.235
55	linalool oxide	C1365191	C <sub>10</sub> H <sub>18</sub> O <sub>2</sub>	170.3	1090.6	795.5	1.236
56	unknown-1	unidentified	/	/	1112.9	971.7	1.389
57	unknown-2	unidentified	/	/	1072.0	672.6	1.893
58	unknown-3	unidentified	/	/	974.8	285.8	1.189
59	unknown-4	unidentified	/	/	1072.3	674.4	1.258
60	unknown-5	unidentified	/	/	1060.1	604.3	1.275
61	unknown-6	unidentified	/	/	1003.4	362.9	1.180
62	unknown-7	unidentified	/	/	1099.7	863.2	1.438
63	unknown-8	unidentified	/	/	1071.7	671.2	1.486
64	unknown-9	unidentified	/	/	891.2	144.8	1.245
65	unknown-10	unidentified	/	/	879.5	133.1	1.278
66	unknown-11	unidentified	/	/	978.3	294.1	1.556
67	unknown-12	unidentified	/	/	957.9	249.2	1.103
68	unknown-13	unidentified	/	/	965.4	264.8	1.295
69	unknown-14	unidentified	/	/	963.7	261.1	1.403

octen-3-ol, safranal, ethyl isobutyrate, 2-heptenal, 1,3-butanediol, isobutyl butyrate, ethyl 2-methylpentanoate, 3-octen-1-ol, methyl benzoate, 2-propanol and 2,4-octadienal. Among them, 2-propanol, 2-heptenal and methyl benzoate in Kerman showed a relatively high

content than those in Shiraz. The other VOCs with significant differences including safranal were high in saffron samples from Shiraz. Safranal, accounting for 60–70 % of the volatile oil in saffron, is the main volatile component affecting the aroma of saffron. (Rezaee & Hosseinzadeh,



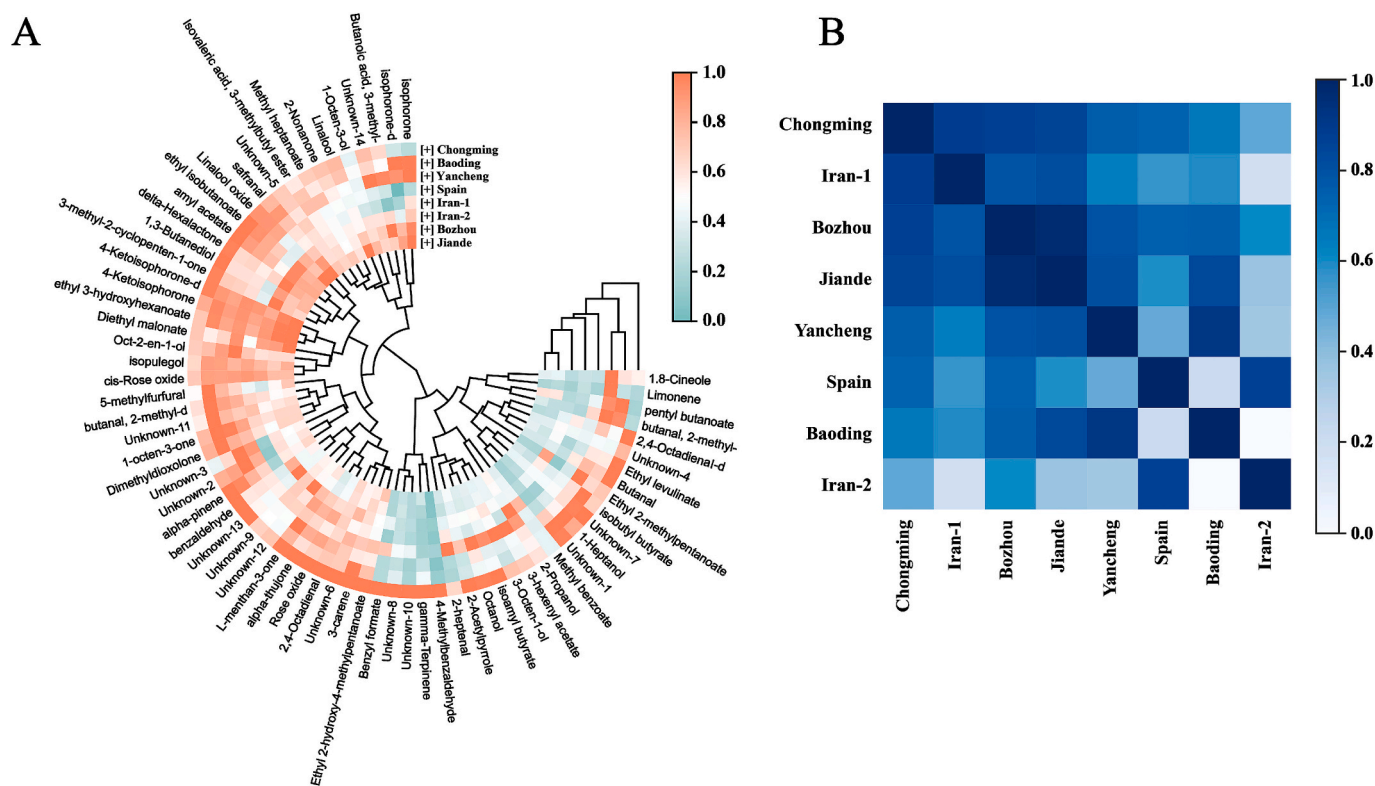


**Fig. 4.** (A) Hierarchical cluster analysis of VOCs in saffron samples from 8 different origins; (B) Correlation analysis of 8 different saffron origins.

**2013)** The quality of saffron is closely related to the volatile compounds including safranal. Hence, the difference of safranal in saffron from Iran Shiraz and Kerman might be contributed to several factors including origins, processing methods and storage conditions. The different climate, soil, planting methods, field fertility and other external factors have a significant impact on the formation of plant quality and the effective ingredient content of metabolites in saffron. (Yang et al., 2018) As shown in Fig. 4A, the content of VOCs in saffron from different origins was different, this may be due to planting method and planting soil environment. According to environmental characteristics, different localities have explored specific cultivation modes according to local conditions. For example, Chongming have overcome the continuous cropping disease of saffron by means of 'water and drought rotation'. Zhejiang areas applied the 'fruit tree saffron' interplanting mode. The soil of Jiande is sticky, rigid and airtight, while the soil of Bozhou is relatively high in sand content, loose and breathable, and not easy to accumulate water. The sandy soil selected by Chongming was more suitable for the growth of saffron seed bulbs and reasonable use of bactericides to carry out the disinfection of saffron bulbs, which is conducive to the accumulation of nutrients and effectively reducing the occurrence of saffron diseases.

In order to further analyze the characterization of VOCs in saffron, the correlation heatmap among different origins of saffron was generated. As shown in Fig. 4B, correlation and difference could be found in the correlation heatmap of different origins. Strong relationships could be found among saffron samples from Chongming, Iran-Kerman, Bozhou and Jande. In addition, among all the saffron origins in China, Bozhou showed a closer correlation to Iran-Shiraz, Iran-Kerman and Spain. We suspected that this may be due to the cultivation method of saffron. The production and processing of saffron in Bozhou referred to traditional methods in foreign countries: directly cultivate and harvest it in the fields. (Ghorbani & Koocheki, 2017) In addition, strong relationships also could be observed between origins of Jiande and Baoding, Yancheng and Baoding, Spain and Iran-Shiraz. In addition to the above-mentioned strong relationships, weak correlations could also be found

in the heatmap. For example, the correlation between Baoding and Iran-Shiraz, Iran-Shiraz and Iran-Kerman, Spain and Baoding. Besides, Iran-Shiraz showed the weakest correlation with other origins, except for Spain. It has been reported that the quality of saffron is closely related to the cultivation temperature, climate, production process, soil condition, storage environment, drying method and other factors. The profiling results of VOCs in saffron from different origins detected by HS-GC-IMS might provide new insights for the illustration of basal origin and characterization of aromatic compounds.

### 3.5. Convolutional neural network for the prediction of saffron origins and the authentication of saffron

In the early exploration of our work, Principal Component Analysis (PCA) was performed to classify and predict the origins of saffron. However, as shown in Fig. S-2, the average classification accuracy was about 61 %, which means these 8 origins could not be distinguished finely by PCA. Only saffron samples from Chongming production area achieved a relatively high accuracy of 79 %. Other origins like Bozhou, Baoding and Yancheng showed the accuracy under 60 %, which brought out obstacles in the classification of origins. In addition, support vector machine (SVM) was also used to classify the origins of saffron. As shown in Fig. S-3, the prediction accuracy of saffron origins by SVM was about 71 % with relatively high accuracy in identifying Yancheng and Spain. However, there are still challenges in utilizing SVM for accurate classification prediction of all saffron origins. For example, the prediction accuracy of saffron origins like Baoding, Bozhou and Chongming were 58 %, 44 % and 54 %. Considering that the direct results of GC-IMS were the heatmaps including rich data information like the retention time, drift time and mass intensity, a novel classification and prediction strategy based on GC-IMS images were emerged. Once the information in the heat map is directly mined and utilized to classify and predict the origin of saffron, not only can data preprocessing be reduced to ensure the speed of prediction, but also the loss of data features during dimensionality reduction can be reduced.

With the advantages of minimal data preprocessing and accurate automatic feature extraction capability, convolutional neural network (CNN) has been regarded as one of the most outstanding algorithms in the deep learning field. (Li, Liu, Yang, Peng, & Zhou, 2022) Compared with traditional classification algorithms, CNN possess a small number of parameters, low computational complexity, fast training speed, as well as being suitable for image processing. For the purpose of developing a universal method of predicting the saffron origins, a CNN model was established. Firstly, the data were augmented using various rigid transformations and the addition of confounding data. Finally, 100 GC-IMS images for each class and a total of 800 GC-IMS images of saffron origins were obtained. Fig. 5A showed the structure of our CNN model, which was composed of two modules: feature extraction part and classification part. The feature extraction part was composed by two convolutional layers and one pooling layer. As shown in Fig. 5A, a series of diverse convolutional kernels perform convolution operations on pixels in the input GC-IMS images, which happened in each convolutional layer. The input shape for the first convolutional layer was (224, 224, 3), representing an image with height, width, and three-color channels. Then, the feature reflections of the input GC-IMS images were extracted benefited by the robust feature-extracting capability of the convolutional layers. Such result might be attributed to the fact that the size of input GC-IMS images was much larger than that of convolutional kernel. Convolutional kernel can effectively decrease the number of weights needed for neural network learning and is conducive to the optimization of the entire model. In the second step, the features obtained were input into the classification part, which was composed by multiple fully-connected layers. Each input feature was considered as a neuron and was connected to all output neurons. Features obtained from convolutional layers could be maximally covered by the fully-connected layer. Finally, the classification results were acquired. The output classification results of this work include 8 different origins and 1 counterfeit result.

The GC-IMS data set used for CNN training contained 900 fingerprint images including 100 images for each class. As shown in Fig. 5B, 70 % of

the GC-IMS data set was used as training data set and 30 % of the GC-IMS was used as testing data set. Fig. 5C displayed the loss and accuracy of train data and validation data of the established CNN model in each training epoch. The losses of the train and validation data reduced rapidly from 0 to 20 epoch, and gradually trended to be stable at 15 epoch. When it comes to the accuracy of the train and validation data, the accuracy rate rose abruptly from 0 to 15 epoch and achieved stable and relatively high accuracy (about 95 %) at 18 epoch. Finally, the training process was set to 18 epoch for maintaining the balance between the accuracy of the prediction of our CNN model and the loss of the data.

With the application of our established CNN model, the prediction results all showed a high accuracy about 90 %. As shown in Fig. 5D, the saffron samples belonging to Spain were predicted with the highest accuracy of 94 %. The accuracies of saffron from Baoding, Iran-Shiraz, Iran-Kerman, and Yancheng were all over 90 % with our developed CNN model. Among them, saffron samples from Jiande and Bozhou showed the lowest accuracy with 83 % and 84 %. This result could be mutually confirmed with the correlation analysis in Fig. 4B. Excessive similarity may be one of the reasons for the relatively low accuracy of saffron prediction in Jiande and Bozhou. Given that the advantage of CNN is that the larger the data sample size, the accuracy of classification will increase. In the future, expanding the sample size of GC-IMS for Bozhou and Jiande saffron will further improve the accuracy of classification prediction.

In addition, the established CNN model also held the ability of identifying counterfeit saffron. Currently, due to the fact that the yield of saffron was limited by the extremely strict growth environment and cultivation methods, the price of saffron is especially high and hard to meet the surge of market demand. This fact bring out the illegal adulteration and substitution happened in the market for profit. (Rocchi et al., 2019) The most frequently used adulterants are dried *Carthamus tinctorius* L. (safflower), *Zea mays* L. (Corn Stigma) and turmeric powder. (Farag, Hegazi, Dokhalahy, & Khattab, 2020) These issues might severely disrupt the market and undermine the public's belief in the high

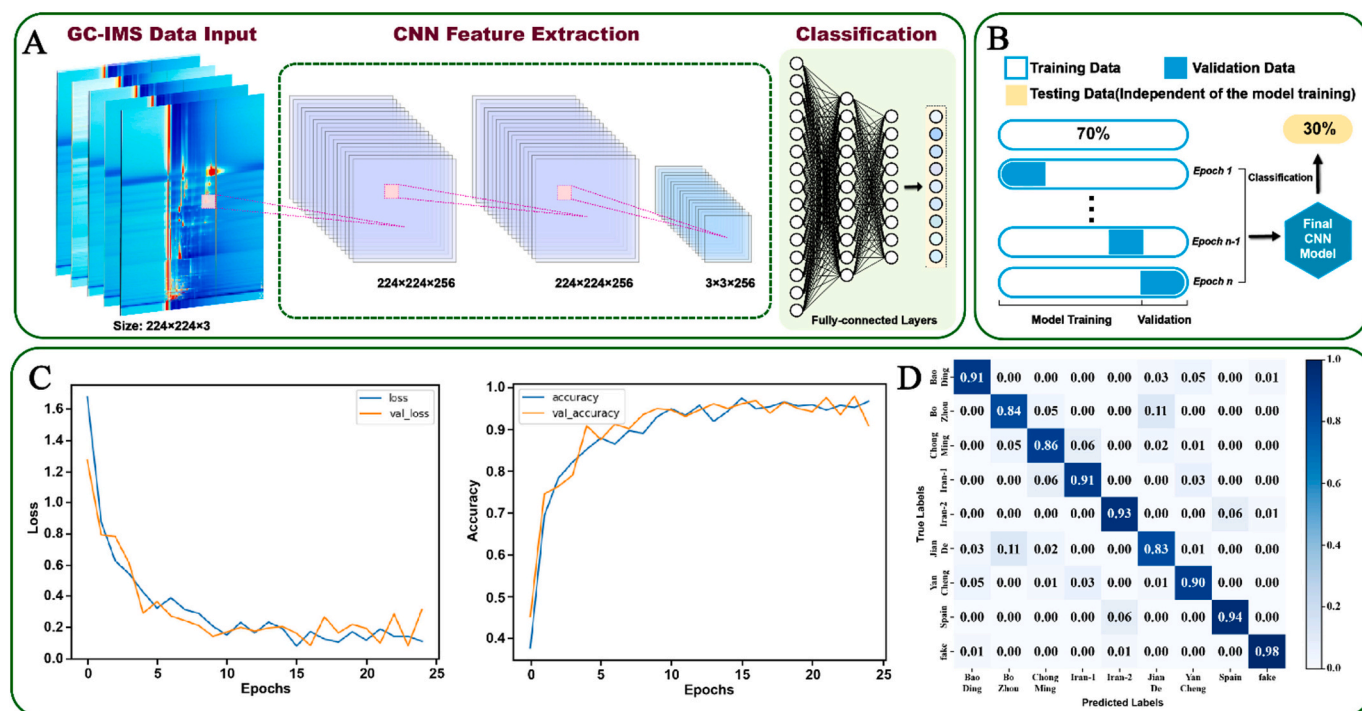


Fig. 5. (A) Schematic diagram of the structure of the established CNN model for the prediction of saffron origins and adulterated samples; (B) Schematic diagram of the training and testing process of the established CNN model. (C) The loss and accuracy of train data and validation data in each epoch during the training process. (D) The prediction result of origins and adulterated samples of saffron by the established CNN model.



nutritional value of saffron. Therefore, a strategy for judging the authenticity of saffron in a rapid and objective way is of great importance. Herein, five kinds of adulterants were gathered: safflower, corn stigma, stamen of saffron, the mixture of saffron and corn stigma, an unknown plant. As shown in Fig. 5D, the accuracy of authentication of saffron could reach 98 % with the application of the CNN model. This result also confirmed that the established CNN model possessed the ability of distinguishing the authenticity of saffron.

#### 4. Conclusion

In this work, a strategy combined with HS-GC-IMS and CNN was used for the characterization and authentication of saffron. Since HS-GC-IMS possess the advantage of simple preprocessing, high sensitivity and multidimensional analysis, 69 VOCs including 7 groups of isomers were detected directly in saffron samples. Hierarchical cluster analysis and correlation analysis were performed to unravel the relationship among different VOCs and origins. Then, a prediction model for classifying saffron origins was developed based on CNN, which accepted GC-IMS images directly as input data. Compared with traditional methods, CNN achieved higher classification and predication accuracy, minimal data preprocessing and accurate automatic feature extraction. The average prediction accuracy of saffron origin reached about 90 %. In addition, the established CNN model was also suitable for the identification of counterfeit saffron with the accuracy of 98 %, which was firstly reported for authentication of saffron samples by CNN combined with HS-GC-IMS. Increasing the amount of data used for CNN classification can improve the model's generalization ability, thereby enhancing prediction accuracy. With the continuous increase of saffron sample detection volume, the strategy proposed in this work would be an important and powerful complement for the characterization and authentication of saffron.

#### CRedit authorship contribution statement

**Yingjie Lu:** Writing – original draft, Supervision, Methodology, Investigation, Data curation. **Chi Zhang:** Validation, Formal analysis, Data curation. **Kunmiao Feng:** Validation, Resources, Methodology. **Jie Luan:** Supervision. **Yuqi Cao:** Methodology, Data curation. **Khalid Rahman:** Supervision. **Jianbo Ba:** Writing – review & editing, Supervision. **Ting Han:** Writing – review & editing, Supervision, Funding acquisition. **Juan Su:** Writing – review & editing, Supervision, Methodology.

#### Declaration of competing interest

The authors declare that they have no known competing financial interests or personal relationships that could have appeared to influence the work reported in this paper.

#### Acknowledgements

This study was supported by National Natural Science Foundation of China (No. 82174091) and Shanghai Pujiang Program (No. 18PJJD061), “Action Plan for Scientific and Technological Innovation of Sustainable Development”, Chongming District of Shanghai (CK2021-03).

#### Appendix A. Supplementary data

Supplementary data to this article can be found online at <https://doi.org/10.1016/j.fochx.2024.101981>.

#### Data availability

Data will be made available on request.

#### References

- Ahrazem, O., Rubio-Moraga, A., Nebauer, S. G., Molina, R. V., & Gómez-Gómez, L. (2015). Saffron: Its Phytochemistry, developmental processes, and biotechnological prospects. *Journal of Agricultural and Food Chemistry*, 63(40), 8751–8764. <https://doi.org/10.1021/acs.jafc.5b03194>
- Amirvaresi, A., Nikounezhad, N., Amirahmadi, M., Daraei, B., & Parastar, H. (2021). Comparison of near-infrared (NIR) and mid-infrared (MIR) spectroscopy based on chemometrics for saffron authentication and adulteration detection. *Food Chemistry*, 344, Article 128647. <https://doi.org/10.1016/j.foodchem.2020.128647>
- Amirvaresi, A., Rashidi, M., Kamyar, M., Amirahmadi, M., Daraei, B., & Parastar, H. (2020). Combining multivariate image analysis with high-performance thin-layer chromatography for development of a reliable tool for saffron authentication and adulteration detection. *Journal of Chromatography A*, 1628, Article 461461. <https://doi.org/10.1016/j.chroma.2020.461461>
- Anastasaki, E., Kanakis, C., Pappas, C., Maggi, L., del Campo, C. P., Carmona, M., & Polissiou, M. G. (2009). Geographical differentiation of saffron by GC-MS/FID and chemometrics. *European Food Research and Technology*, 229(6), 899–905. <https://doi.org/10.1007/s00217-009-1125-x>
- Aspromonte, J., Giacompo, G., Wolfs, K., & Adams, E. (2020). Headspace gas chromatography for the determination of volatile methylsiloxanes in personal care products. *Analytical and Bioanalytical Chemistry*, 412(11), 2537–2544. <https://doi.org/10.1007/s00216-020-02478-y>
- Avgerinos, K. I., Vrysis, C., Chaitidis, N., Kolotsiou, K., Myserlis, P. G., & Kapogiannis, D. (2020). Effects of saffron (*Crocus sativus* L.) on cognitive function. A systematic review of RCTs. *Neurological Sciences*, 41(10), 2747–2754. <https://doi.org/10.1007/s10072-020-04427-0>
- Brendel, R., Schwolow, S., Rohn, S., & Weller, P. (2021). Volatilomic profiling of Citrus juices by dual-detection HS-GC-MS-IMS and machine learning—An alternative authentication approach. *Journal of Agricultural and Food Chemistry*, 69(5), 1727–1738. <https://doi.org/10.1021/acs.jafc.0c07447>
- Capitain, C., & Weller, P. (2021). Non-targeted screening approaches for profiling of volatile organic compounds based on gas chromatography-ion mobility spectroscopy (GC-IMS) and machine learning. *Molecules*, 26(18). <https://doi.org/10.3390/molecules26185457>
- D'Archivio, A. A., Di Pietro, L., Maggi, M. A., & Rossi, L. (2018). Optimization using chemometrics of HS-SPME/GC-MS profiling of saffron aroma and identification of geographical volatile markers. *European Food Research and Technology*, 244(9), 1605–1613. <https://doi.org/10.1007/s00217-018-3073-9>
- Denia, A., Esteve-Turrillas, F. A., & Armenta, S. (2022). Analysis of drugs including illicit and new psychoactive substances in oral fluids by gas chromatography-drift tube ion mobility spectrometry. *Talanta*, 238, Article 122966. <https://doi.org/10.1016/j.talanta.2021.122966>
- Di Donato, F., D'Archivio, A. A., Maggi, M. A., & Rossi, L. (2021). Detection of plant-derived adulterants in saffron (*Crocus sativus* L.) by HS-SPME/GC-MS profiling of volatiles and Chemometrics. *Food Analytical Methods*, 14(4), 784–796. <https://doi.org/10.1007/s12161-020-01941-x>
- Farag, M. A., Hegazi, N., Dokhalahy, E., & Khattab, A. R. (2020). Chemometrics based GC-MS aroma profiling for revealing freshness, origin and roasting indices in saffron spice and its adulteration. *Food Chemistry*, 331, Article 127358. <https://doi.org/10.1016/j.foodchem.2020.127358>
- Feng, D., Wang, J., He, Y., Ji, X.-J., Tang, H., Dong, Y.-M., & Yan, W.-J. (2021). HS-GC-IMS detection of volatile organic compounds in Acacia honey powders under vacuum belt drying at different temperatures. *Food Science & Nutrition*, 9(8), 4085–4093. <https://doi.org/10.1002/fsn3.2364>
- Ge, S., Chen, Y., Ding, S., Zhou, H., Jiang, L., Yi, Y., & Wang, R. (2020). Changes in volatile flavor compounds of peppers during hot air drying process based on headspace-gas chromatography-ion mobility spectrometry (HS-GC-IMS). *Journal of the Science of Food and Agriculture*, 100(7), 3087–3098. <https://doi.org/10.1002/jsfa.10341>
- Ghanbari, J., Khajoei-Nejad, G., Erasmus, S. W., & van Ruth, S. M. (2019). Identification and characterisation of volatile fingerprints of saffron stigmas and petals using PTR-TOF-MS: Influence of nutritional treatments and corn provenance. *Industrial Crops and Products*, 141, Article 111803. <https://doi.org/10.1016/j.indcrop.2019.111803>
- Ghorbani, R., & Koocheki, A. (2017). Sustainable cultivation of saffron in Iran. In E. Lichtfouse (Ed.), *Sustainable agriculture reviews* (pp. 169–203). Cham: Springer International Publishing.
- Gu, S., Zhang, J., Wang, J., Wang, X., & Du, D. (2021). Recent development of HS-GC-IMS technology in rapid and non-destructive detection of quality and contamination in Agri-food products. *TrAC Trends in Analytical Chemistry*, 144, Article 116435. <https://doi.org/10.1016/j.trac.2021.116435>
- Karabagias, I. K., Koutsoumpou, M., Liakou, V., Kontakos, S., & Kontominas, M. G. (2017). Characterization and geographical discrimination of saffron from Greece, Spain, Iran, and Morocco based on volatile and bioactivity markers, using chemometrics. *European Food Research and Technology*, 243(9), 1577–1591. <https://doi.org/10.1007/s00217-017-2866-6>
- Kumar, A., Devi, M., Kumar, R., & Kumar, S. (2022). Introduction of high-value *Crocus sativus* (saffron) cultivation in non-traditional regions of India through ecological modelling. *Scientific Reports*, 12(1), 11925. <https://doi.org/10.1038/s41598-022-15907-y>
- Kumari, L., Jaiswal, P., & Tripathy, S. S. (2021). Various techniques useful for determination of adulterants in valuable saffron: A review. *Trends in Food Science & Technology*, 111, 301–321. <https://doi.org/10.1016/j.tifs.2021.02.061>
- Leng, P., Hu, H.-W., Cui, A.-H., Tang, H.-J., & Liu, Y.-G. (2021). HS-GC-IMS with PCA to analyze volatile flavor compounds of honey peach packaged with different

- preservation methods during storage. *LWT*, 149, Article 111963. <https://doi.org/10.1016/j.lwt.2021.111963>
- Li, M., Yang, R., Zhang, H., Wang, S., Chen, D., & Lin, S. (2019). Development of a flavor fingerprint by HS-GC-IMS with PCA for volatile compounds of *Tricholoma matsutake* singer. *Food Chemistry*, 290, 32–39. <https://doi.org/10.1016/j.foodchem.2019.03.124>
- Li, Z., Liu, F., Yang, W., Peng, S., & Zhou, J. (2022). A survey of convolutional neural networks: Analysis, applications, and prospects. *IEEE Transactions on Neural Networks and Learning Systems*, 33(12), 6999–7019. <https://doi.org/10.1109/TNNLS.2021.3084827>
- Maggi, L., Carmona, M., Zalacain, A., Kanakis, C. D., Anastasaki, E., Tarantilis, P. A., & Alonso, G. L. (2010). Changes in saffron volatile profile according to its storage time. *Food Research International*, 43(5), 1329–1334. <https://doi.org/10.1016/j.foodres.2010.03.025>
- Masoomi, S., Sharifi, H., & Hemmateenejad, B. (2024). An optical-nose device based on fluorescent nanomaterials sensor array for authentication of saffron. *Sensors and Actuators B: Chemical*, 405, Article 135365. <https://doi.org/10.1016/j.snb.2024.135365>
- Naim, N., Guirrou, I., Fauconnier, M.-L., Hafida, H., Tahiri, A., Madani, I., & Ennahli, S. (2023). Chemical, biochemical and volatile profiles of saffron (*Crocus sativus* L.) from different growing areas of Morocco. *JSAFA reports*, 3(5), 233–247. <https://doi.org/10.1002/jsf2.114>
- Pandita, D. (2021). Chapter 14 - saffron (*Crocus sativus* L.): Phytochemistry, therapeutic significance and omics-based biology. In T. Aftab, & K. R. Hakeem (Eds.), *Medicinal and aromatic plants* (pp. 325–396). Academic Press.
- Pu, D., Cao, B., Xu, Z., Zhang, L., Meng, R., Chen, J., & Zhang, Y. (2025). Decoding of the enhancement of saltiness perception by aroma-active compounds during Hunan Larou (smoke-cured bacon) oral processing. *Food Chemistry*, 463, Article 141029. <https://doi.org/10.1016/j.foodchem.2024.141029>
- Pu, D., Duan, W., Huang, Y., Zhang, Y., Sun, B., Ren, F., & Tang, Y. (2020). Characterization of the key odorants contributing to retronasal olfaction during bread consumption. *Food Chemistry*, 318, Article 126520. <https://doi.org/10.1016/j.foodchem.2020.126520>
- Rawat, W., & Wang, Z. (2017). Deep convolutional neural networks for image classification: A comprehensive review. *Neural Computation*, 29(9), 2352–2449. [https://doi.org/10.1162/neco\\_a\\_00990](https://doi.org/10.1162/neco_a_00990)
- Rezaee, R., & Hosseinzadeh, H. (2013). Saffron: From an aromatic natural product to a rewarding pharmacological agent. *Iranian Journal of Basic Medical Sciences*, 16(1), 12–26. <https://doi.org/10.22038/IJBMS.2013.244>
- Rocchi, R., Mascini, M., Faberi, A., Sergi, M., Compagnone, D., Di Martino, V., & Pittia, P. (2019). Comparison of IRMS, GC-MS and E-nose data for the discrimination of saffron samples with different origin, process and age. *Food Control*, 106, Article 106736. <https://doi.org/10.1016/j.foodcont.2019.106736>
- Rubert, J., Lacina, O., Zachariasova, M., & Hajslova, J. (2016). Saffron authentication based on liquid chromatography high resolution tandem mass spectrometry and multivariate data analysis. *Food Chemistry*, 204, 201–209. <https://doi.org/10.1016/j.foodchem.2016.01.003>
- Sobolev, A. P., Carradori, S., Capitani, D., Vista, S., Trella, A., Marini, F., & Mannina, L. (2014). Saffron samples of different origin: An NMR study of microwave-assisted extracts. *Foods*, 3(3), 403–419. <https://doi.org/10.3390/foods3030403>
- Sun, X., Gu, D., Fu, Q., Gao, L., Shi, C., Zhang, R., & Qiao, X. (2019). Content variations in compositions and volatile component in jujube fruits during the blacking process. *Food Science & Nutrition*, 7(4), 1387–1395. <https://doi.org/10.1002/fsn3.973>
- Chen, S.-A., Wang, X., Zhao, B., Yuan, X., & Wang, Y. (2003). Production of crocin using *Crocus sativus* callus by two-stage culture system. *Biotechnology Letters*, 25(15), 1235–1238. <https://doi.org/10.1023/A:1025036729160>
- Yang, L., Wen, K.-S., Ruan, X., Zhao, Y.-X., Wei, F., & Wang, Q. (2018). Response of plant secondary metabolites to environmental factors. *Molecules*, 23(4), 762. <https://doi.org/10.3390/molecules23040762>
- Yang, Y., Wang, B., Fu, Y., Shi, Y.-G., Chen, F.-I., Guan, H.-N., & Zhang, N. (2021). HS-GC-IMS with PCA to analyze volatile flavor compounds across different production stages of fermented soybean whey tofu. *Food Chemistry*, 346, Article 128880. <https://doi.org/10.1016/j.foodchem.2020.128880>
- Zhou, S., Feng, D., Zhou, Y., Zhao, J., Zhao, J., Guo, Y., & Yan, W. (2022). HS-GC-IMS detection of volatile organic compounds in cistanche powders under different treatment methods. *LWT*, 165, Article 113730. <https://doi.org/10.1016/j.lwt.2022.113730>
- Zhou, Y., Wang, D., Duan, H., Zhou, S., Guo, J., & Yan, W. (2023). Detection and analysis of volatile flavor compounds in different varieties and origins of goji berries using HS-GC-IMS. *LWT*, 187, Article 115322. <https://doi.org/10.1016/j.lwt.2023.115322>